

Received June 25, 2020, accepted July 10, 2020, date of publication July 20, 2020, date of current version July 30, 2020.

Digital Object Identifier 10.1109/ACCESS.2020.3010409

# DP and DS-LCD: A New Lane Change Decision Model Coupling Driver's Psychology and Driving Style

ZHIHUI LI<sup>ID</sup>, CONG WU<sup>ID</sup>, PENGFEI TAO<sup>ID</sup>, JING TIAN<sup>ID</sup>, AND LIN MA<sup>ID</sup>

School of Transportation, Jilin University, Changchun 130022, China

Corresponding author: Pengfei Tao (taopengfei@jlu.edu.cn)

This work was supported in part by the National Natural Science Foundation of China under Grant 51705196, and in part by the Science and Development Project of Jilin Province under Grant 20190201107JC.

**ABSTRACT** Lane-Changing Decision (LCD) behavior is complex, dangerous, and varied by the Driver's Psychology (DP) and Driving Style (DS). For lacking the consideration of DP and DS, the existing LCD models cannot predict the LCD process varying with the drivers and traffic conditions accurately. To deal with the problems, a new LCD model coupling DP and DS, named DP&DS-LCD, is put forward. In the model, a psychological field model is constructed to represent the DP effect on the scene vehicles. And then, *K*-means and *K*-Nearest Neighbor (KNN) algorithm are respectively adopted in learning and recognition phases to recognize the current driving style pattern. Finally, based on the DP and DS, the multi-Grained Cascade Forest (gcForest) algorithm is applied to predict the LCD behavior. In experiments, DP&DS-LCD is compared with other three LCD models by using the opening I-80 database from Next Generation Simulation project (NGSIM). And the results showed that the DP&DS-LCD model achieved the best performance. Therefore, the DP&DS-LCD model is effective and could provide support for the decision of autonomous vehicles by predicting the surrounding vehicles' Lane-Changing (LC) behavior.

**INDEX TERMS** Autonomous vehicles, driver's psychology, driving style, lane change decision.

## I. INTRODUCTION

With the development of autonomous driving technology, the mixed driving of autonomous vehicles and artificial vehicles will become a common situation in the future. In order to ensure the safe driving of autonomous vehicles, it is important to predict the LC behavior of the surrounding artificial vehicles accurately.

Generally speaking, LC process contains LCD and LC execution stages, as shown in Fig. 1. According to the LC purpose, LCD can be split into Mandatory LCD (MLCD) and Discretionary LCD (DLCD). For DLCD, it is implemented to change the vehicle's motion process from the current lane to the target lane for the better driving speed. Here, the LCD problem on DLCD is addressed. As usual, LCD procedure could be divided into four stages: (1) LC intention generation; (2) target lane selection; (3) LC condition judgment; (4) LC execution. The LC intention is generated by drivers and

The associate editor coordinating the review of this manuscript and approving it for publication was Chao Yang<sup>ID</sup>.

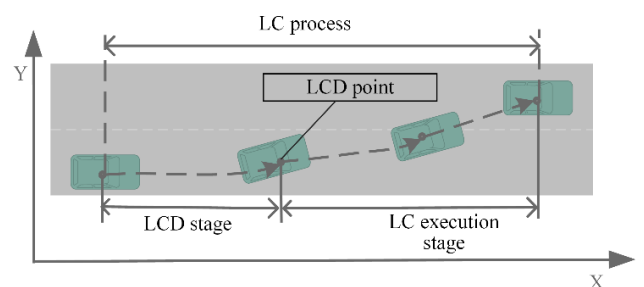


FIGURE 1. Diagram of the LC process.

influenced by many complex factors, such as DP, DS, driving circumstances, etc. However, the driver's surrounding circumstances could also produce the psychological stimulation to the driver, which leads to the change of driver's psychological state. Accordingly, to describe LCD behavior accurately, the effect of DP and DS should be considered, and the unified form of DP effect could be quantified by driver's surrounding circumstances.

Currently, many methods have been presented to predict LCD (e.g. rule-based [1]–[3], fuzzy reasoning [4]–[6], data-driven algorithm [7]–[10], etc.). However, these studies focused on modeling the surrounding traffic conditions on LC vehicles, and lacked consideration of DP and DS. This may ignore the driver's subjective effect on the LCD. Some studies have added the DP into LC studies [11], and the DP is generally obtained by questionnaire survey or physiological tester. But the DP evaluation result is a qualitative or indirect index by these methods, which cannot describe the DP changes firsthand and quantitatively. Furthermore, DS also affects the LC strategy. Some researchers have taken the DS into the LC model [12], [13]. And there are many driving style classification models [14]–[16]. But these methods usually extract the driving style characteristics through a large number of trajectory data, and then use unsupervised learning method to classify driving styles. There is a problem with these classification methods. That is once the driver's driving style is obtained from the historical data, it will not change. However, the driving style is influenced by the traffic conditions, external environment, etc., and it is not invariable. Therefore, these classification models cannot get the driver's current driving style.

To solve the above issues, a novel LCD model from the driver's perspective is developed, by integrating the DP and DS, called DP&DS-LCD. The psychological field model is adopted to quantify the driver's mental state, and it could depict the driver's psychological pressure caused by the surrounding vehicles in the driving process. Then, a driving style recognition system is designed, which includes offline training stage and online recognition stage. Offline learning phase uses the vehicles' historical trajectories and  $K$ -means to establish the mapping relationship between drivers' characteristics and driving styles. The online identification stage is to judge the driver's current driving style based on the real-time trajectories and KNN.

Furthermore, in order to provide the real-time decision support for autonomous vehicles, it is necessary to obtain the surrounding vehicles' information timely. The Vehicle-to-Vehicle (V2V) communication technology enables vehicles to send information to each other, such as position and speed. Therefore, autonomous vehicles could obtain the real-time information of surrounding vehicles in V2V environment, and then could predict the LC behavior of the surrounding vehicles with LCD model, so as to plan their behaviors, as shown in Fig. 2.

The rest of the paper is arranged as follows: section 2 reviews the related works about LCD models; section 3 gives the details of DP&DS-LCD model, which includes the quantified expression of the DP pressure with psychological field model, DS classification algorithm, and LCD prediction; section 4 discusses and analyzes the experimental results; section 5 is the summary of the article and discussion.

The main contributions of this article are listed as follows.

1) A novel LCD model is proposed by coupling the DP and DS.

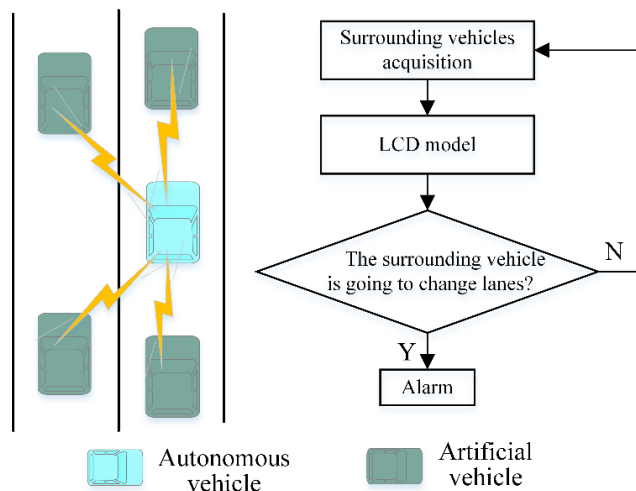


**FIGURE 2.** Framework of autonomous vehicle decision-making in V2V environment.

2) A DP quantification method is present in this paper, which is based on the driver's psychological field.

3) Developing a DS classification model which could recognize the driver's current driving style.

## II. RELATED WORKS

The LCD behavior has been widely studied by many researchers. And the current LCD researches can be divided into three categories: rules-based, fuzzy logical, and data-driven.

The rule-based LCD model deduces whether the vehicle will perform LC at a certain position by formulating LC rules. Gipps [1] firstly put forward a rule-based model which considered six factors: safe distance, the location of permanent obstructions, the presence of transit lanes, the intended turning movement of the driver, the presence of heavy vehicles, and the speed of the vehicle. Kind and Kesting [2] developed a general LCD model named MOBIL (Minimizing Overall Braking Induced by Lane Changes). The model formulated a set of LC rules which mainly considered the lane utility and LC risk. Wang *et al.* [3] proposed a reinforcement learning method based on the LC rules, which was used to provide support for autonomous driving decision. This model mainly considered the safety of self-driving vehicles.

The fuzzy logic model can better deal with the uncertainty in driving decision, and it consists of several if-then rules. For example, Das and Bowles [4] proposed a gap acceptance model based on the fuzzy logic, which mainly considered the speed of the front and rear vehicle in the target lane, and the distance between them and the target vehicle. Balal *et al.* [5] developed a LCD model based on the fuzzy reasoning system, which took the distance between the main vehicle and the host vehicle as the LCD factors. Moridpour *et al.* [6] designed two and three fuzzy sets to predict the LCD behavior of heavy vehicle.

With the emergence of artificial intelligence algorithms, there are numerous LCD models based on data-driven. There is no specific formula for the data-driven LCD model, which learns the characteristics of LCD samples through a large amount of data. Coskun *et al.* [7] proposed a LCD model by integrating the fuzzy logic and Markov Decision Process (MDP). And they have verified the model effectiveness under several driving scenarios. Yuan *et al.* [8] selected the distance between the vehicle and the lane line, the longitudinal velocity, and lateral velocity of the vehicle as the input of LCD model. And they used Hidden Markov Model (HMM) to train and test the model. Zhang *et al.* [9] selected the location information of the target vehicle and the six surrounding vehicles as the model input. And they proposed a Hybrid Retraining Constraint (HRC) training to optimize the Long Short Term Memory (LSTM) algorithm, then they used this method to train the LC model. Xie *et al.* [10] selected the speed and location information of the target vehicle, the front car on the present lane, and the front car and the rear car on the target lane as the model input. Then they used Depth Belief Network (DBN) to predict the LCD behavior.

Although the above LCD models are based on different modeling methods, they are similar in the selection of LCD factors. These researches mainly concentrated on the surrounding traffic conditions, which are generally the position and speed information of some specific vehicles. However, this would ignore the driver's direct role for LCD. The LCD behavior is mostly affected by the DP and DS. Moreover, drivers' heterogeneity determines the difference of LCD strategies. And some studies have taken the driver's characteristics into the LC model. Li *et al.* [12] used questionnaire survey to get the driver's driving style and took it into the LC intention model. The results showed that distinguishing driving styles could improve the prediction accuracy significantly. This is different from our work. Because our method doesn't need manually define the driving style and all driver styles are learned from trajectory data. Eftekhari and Ghatee [14] utilized the vehicles' trajectories and *K*-means to divide the drivers into three categories, then adopted the multi-layer perceptron to predict the LC behavior. The above methods usually obtained the driving style from the historical trajectory data. And once getting the driver's driving style, it will not change. However, driver's driving style is affected by many factors (e.g. the present traffic conditions, surrounding environment, etc.), and it is not stable. So it may be more accurate to adopt real-time trajectory data to calibrate the current driving style.

To solve the above problems, a DP&DS-LCD model based on the driver's perspective is developed in this study. And the detailed modeling process is illustrated in section III.

### III. DP&DS-LCD MODEL

The DP&DS-LCD model mainly contains three parts, as shown in Fig. 3. Firstly, the driver's psychological field model is used to quantify the DP. It includes the definition of the driver's psychological field, the affect area

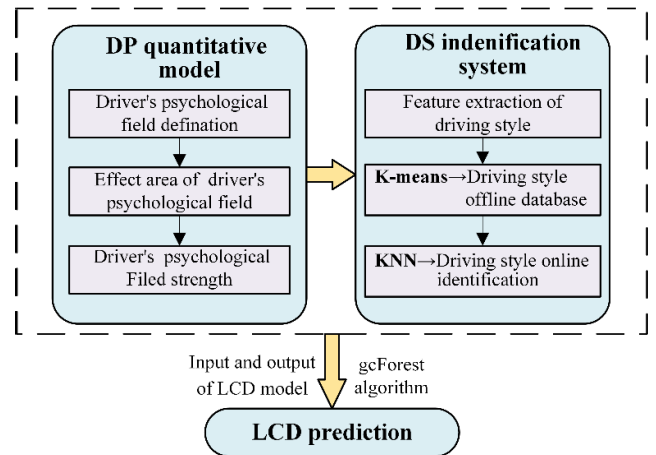


FIGURE 3. Framework of DP&DS-LCD model.

of psychological field under different driving scenarios, and the calculation method of the psychological field strength. Then, in order to get the driver's current driving style, a DS definition system is proposed. And the system includes the driving style offline database and the online recognition. Finally, the DP and the DS are used for LCD prediction. And the gcForest algorithm is adopted to train the model.

#### A. DP QUANTITATIVE METHOD IN DP&DS-LCD MODEL

In order to predict the vehicle's LCD behavior in different traffic situations, it is necessary to model the psychological effect of surrounding vehicles on the driver. The driver's psychological field theory [17]–[19] is used to make a quantitative expression of DP in Car-Following (CF) and LC process. The psychological field source is the driver, and the effect area of the psychological field is determined by the position of the surrounding vehicles which the driver is concerned about. The psychological field strength represents the driver's psychological stress caused by the surrounding vehicles. And the psychological field strength can be obtained, by calculating the sum of the field strength of the vehicles which are in the effect area of driver's mental field.

##### 1) DRIVER'S PSYCHOLOGICAL FIELD MODEL

Driver's attention range for the surrounding traffic circumstances determines the effect area of the psychological field. Because there is a difference in driver's attention range between the CF and LC stage, which means, there is a difference in the effect area of the psychological field. When the vehicle keeps CF, the driver mostly focuses on the preceding vehicles which are in the same driving direction with the vehicle, as shown in Fig. 4. Conversely, a safe gap is needed to find when executing LC. Therefore, the driver's attention is on the vehicles which are on the present lane and target lane, as shown in Fig. 4 (taking left LC as an example).

After the effect area of psychological field is defined, it is needed to determine the basic field strength of an arbitrary point in psychological field. The basic field strength

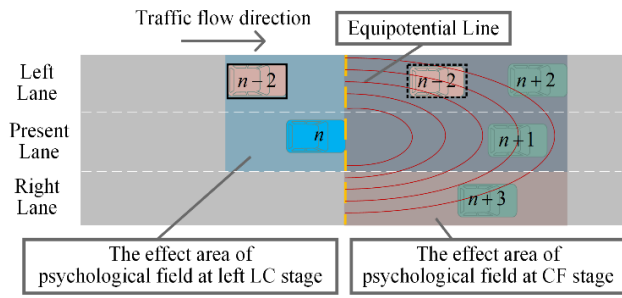


**FIGURE 4.** Illustration of driver's psychological field. Here "n" denotes the host vehicle. "n+1" denotes the vehicle on the present lane. "n-2" and "n+2" denote the vehicles on the left lane. "n+3" denotes the vehicle on the right lane.

represents the psychological pressure of a certain point surrounding the driver, and it is closely related to the time distance from this point to the target vehicle. The smaller the time distance between the point and the target vehicle, the greater the psychological pressure (field strength) generated by the driver. Therefore, there are the negative correlation between the two variables. The basic field strength can be expressed as:

$$Eb_i = \frac{v_i + v_\varepsilon}{d_0} \quad (1)$$

here,  $v_i$  is the speed of target vehicle,  $v_\varepsilon$  is the speed correction.  $d_0$  is the projected distance between the point and the target vehicle in the moving direction of the target vehicle.

The construction of the equipotential line mainly refers to the previous study of our research team [19]. Since the field strength of any position on the equipotential line is the same, the equivalent distance of the point in the moving direction of the target vehicle can be calculated, as (2) shown.

$$d_0 = \frac{d_{(x,y)}}{1 - (1 - \alpha(v_i)) |\sin \theta|} \quad (2)$$

here,  $d_{(x,y)}$  is the distance between any point and the origin (the driver's position).  $\alpha(v_i)$  is the ratio of the distance between the point where the equipotential line intersects the vehicle's moving direction and the origin, and the distance between the point where the equipotential line intersects the direction perpendicular to the vehicle's moving direction and the origin.  $\theta$  is the angle between the vehicle's running direction, and the line from any point on the equipotential line to the origin.

According to (1) and (2), the basic field strength of any point in driver's psychological field could be calculated, as (3) shown.

$$Eb_i = \frac{v_i + v_\varepsilon}{d_{(x,y)}} [1 - (1 - \alpha(v_i)) |\sin \theta|] \quad (3)$$

## 2) CALCULATED METHOD FOR PSYCHOLOGICAL EFFECT OF VEHICLES IN PSYCHOLOGICAL FIELD ON THE DRIVER

As shown in Fig. 5, based on the driver's visual attention mechanism, the driver could see the surrounding vehicle's

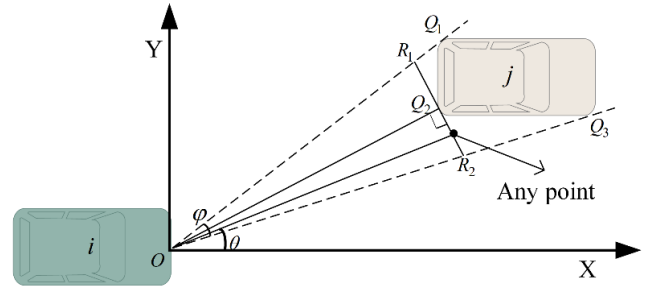


**FIGURE 5.** Visual projection diagram of the surrounding vehicle  $j$  relative to the driver of target vehicle  $i$ .  $\varphi$  is the visual angle.

outline  $Q_1Q_2$  and  $Q_2Q_3$ , which is actually a visual projection line  $R_1R_2$  in driver's eye. Each point on the line  $R_1R_2$  has a basic field, so the first curve integral is adopted to calculate the field intensity.

Set the coordinates of  $R_1$  and  $R_2$  are  $(x_1, y_1)$  and  $(x_2, y_2)$ , then the equation of the line  $R_1R_2$  is:

$$\begin{cases} x = \lambda \\ y = \frac{y_2 - y_1}{x_2 - x_1} \lambda + \frac{y_1 x_2 - y_2 x_1}{x_2 - x_1} \end{cases} \quad (4)$$

The mental field strength of vehicle  $j$  on the driver at time  $t$  is calculated as:

$$\begin{aligned} e_{ij}^t &= \int_{R_1R_2} Eb_i(x, y) ds \\ &= \int_{x_1}^{x_2} Eb_i \left( \lambda, \frac{y_2 - y_1}{x_2 - x_1} (\lambda - x_1) + y_1 \right) \\ &\quad \times \sqrt{1 + \left( \frac{y_2 - y_1}{x_2 - x_1} \right)^2} d\lambda \end{aligned} \quad (5)$$

Let  $\frac{y_2 - y_1}{x_2 - x_1} = h$ ,  $\frac{y_1 x_2 - y_2 x_1}{x_2 - x_1} = b$ , combining with (3), the (5) can be simplified as:

$$\begin{aligned} e_{ij}^t &= (v_i + v_\varepsilon) \sqrt{h^2 + 1} \\ &\quad \times \left\{ \int_{x_1}^{x_2} \frac{1}{\sqrt{\lambda^2 + (h\lambda + b)^2}} d\lambda \right. \\ &\quad \left. - (1 - \alpha(v_i)) \int_{x_1}^{x_2} \frac{|h\lambda + b|}{\lambda^2 + (h\lambda + b)^2} d\lambda \right\} \end{aligned} \quad (6)$$

here, when  $R_1R_2$  is above the  $X$ -axis,  $|h\lambda + b| = h\lambda + b$ ; when  $R_1R_2$  is below the  $X$ -axis,  $|h\lambda + b| = -h\lambda - b$ . Particularly, if  $R_1R_2$  intersects to the  $X$ -axis, the intersection point will be set as  $R_3(x_3, y_3)$ , then  $e_{ij}^t$  is:

$$\begin{aligned} e_{ij}^t &= (v_i + v_\varepsilon) \sqrt{h^2 + 1} \\ &\quad \left\{ \int_{x_1}^{x_3} \frac{1}{\sqrt{\lambda^2 + (h\lambda + b)^2}} d\lambda + \int_{x_3}^{x_2} \frac{1}{\sqrt{\lambda^2 + (h\lambda + b)^2}} d\lambda \right. \\ &\quad \left. - (1 - \alpha(v_i)) \int_{x_1}^{x_3} \frac{h\lambda + b}{\lambda^2 + (h\lambda + b)^2} d\lambda \right. \\ &\quad \left. + (1 - \alpha(v_i)) \int_{x_3}^{x_2} \frac{h\lambda + b}{\lambda^2 + (h\lambda + b)^2} d\lambda \right\} \end{aligned} \quad (7)$$

Attention, the (6) and (7) are valid on the premise of  $x_1 < x_2$ . If the reader is interested in other cases, you can derive it by yourself.

In conclusion, the driver's total field intensity  $e_i^t$  can be expressed as:

$$e_i^t = \sum_{j \in eS_i^t} e_{ij}^t \quad (8)$$

here,  $eS_i^t$  is the effect scope of psychological field of driver  $i$  at time  $t$ .

### B. DS DETERMINATION SYSTEM

Drivers with different driving styles have different preferences for driving speed, acceleration, deceleration, and LC frequency [20], [21]. So the feature vector of driving style can be constructed as:

$$f = \{v, |a|, n_{LC}\} \quad (9)$$

where  $v$ ,  $|a|$ ,  $n_{LC}$  are respectively the vehicle's velocity, absolute acceleration, and LC frequency at unit length.

Nevertheless, driving style is affected by the traffic situations. In different traffic states, the same driver may present diverse driving styles. Therefore, it is necessary to divide the traffic states, and classify the driving styles under the same traffic condition. The traffic state around the driver is termed as Local Dynamic Density (LDD) in this study. The change of driver's psychology comes from the traffic circumstances' stimulation, so the surrounding traffic states could be reflected through the psychological field strength. And there is an equivalence relation between the two. The LDD can be expressed as follows:

$$\rho_i^t = e_i^t \quad (10)$$

here,  $\rho_i^t$  is the LDD perceived by driver  $i$  at time  $t$ .

Since the driving style has a certain stability, this paper supposes that the driver's driving style does not change within  $T$  time-length. And the range of  $T$  is suggested from 3 s to 10 s. Then, statistical indicators are utilized for driving style representation, which include average value and Standard Deviation (SD). Therefore the evaluation indexes of driving style are constructed as:

$$f' = \left\{ v_{mean}^{t-T,t}, v_{SD}^{t-T,t}, |a|_{mean}^{t-T,t}, |a|_{SD}^{t-T,t}, n_{LC}^{t-T,t} \right\} \quad (11)$$

In order to improve the practical operability, a driving style recognition framework is established in this study, which combines the personalized driving characteristics with surrounding traffic circumstances. As described in Fig. 6, the framework includes the driving style offline database and driving style online recognition system. The offline database mainly uses the unsupervised learning algorithm  $K$ -means to establish the mapping relationship between driving behavior features and driving styles. The online identification system can identify the driver's current driving style effectively. Then these two parts will be described in detail.

In Fig. 6, the processing method of the original training dataset and original estimated sample is annotated with “\*”. And the selecting principle for the original data from time  $t-T$  to time  $t$  is: considering the continuity of the traffic state evolution, extracting the continuity range of LDD from time  $t-T$  to time  $t$ , which belongs to the same LDD category and close to time  $t$ , then correspondingly calculating the evaluation indexes. Some symbols in Fig. 6 will be explained,  $k_0$  is the initial cluster number.  $g$  and  $k$  are the number of traffic condition categories and the cluster number of driving styles.  $g'$  is the  $g'$ -th traffic condition, where  $g' \in [1, g]$ .  $G$  and  $K$  are the maximum classification number of traffic conditions and driving styles.  $N$  is the maximum iterations,  $\varepsilon$  is the criteria of stopping iteration. The objective function  $J(c, \mu)$  is defined as:

$$J(c, \mu) = \sum_{i=1}^k \sum_{j=1}^m \left\| c_{ij} - c'_{ij} \right\|^2 \quad (12)$$

here  $c_{ij}$  and  $c'_{ij}$  ( $i \in [1, k], j \in [1, m]$ ) are the  $j$ -th parameters of  $k$ -th cluster in which they are distinguished with each other for computation.

$K$ -means is a commonly used unsupervised classification algorithm, which takes the Euclidean distance to evaluate the similarity between vector quantities. However,  $K$ -means needs to be given a fixed number of clusters, which may lead to the clustering results cannot achieve the desired effect. Therefore, in order to improve the performance of  $K$ -means, the Davies-Bouldin (DB) index is utilized in this paper, which can evaluate the dispersion degree between different clusters. More details please refer to [22]. The DB index is calculated as follows:

$$\bar{R}_k = \frac{1}{k} \sum_{i=1}^k R_i = \frac{1}{k} \sum_{i=1}^k \max_{j \neq i} R_{ij} \quad (13)$$

with

$$R_{ij} = \frac{s(c_i) + s(c_j)}{d(c_i, c_j)} \quad (14)$$

$$s(c_i) = \frac{1}{|c_i|} \sum_{x \in c_i} \|x - \mu_i\| \quad (15)$$

$$d(c_i, c_j) = \|\mu_i - \mu_j\| \quad (16)$$

where  $\bar{R}_k$  is the DB index when the driving styles are divided into  $k$  clusters.  $R_{ij}$  is the similarity between cluster  $i$  and cluster  $j$ .  $s(c_i)/s(c_j)$  is the average distance between the vectors in the cluster  $i/j$  and the center of the cluster  $i/j$ .  $d(c_i, c_j)$  is the distance between cluster  $i$  and cluster  $j$ , and Euclidean distance is adopted in this paper.  $x$  is the individual of cluster  $i$ .  $|c_i|$  is the number of individuals of cluster  $i$ .  $\mu_i$  and  $\mu_j$  are the cluster center of cluster  $i$  and cluster  $j$ .

After the offline database of driving style is established, supervised learning algorithm KNN is adopted to identify the driver's current driving style. The core of KNN algorithm is to estimate the category of samples by comparing the similarity among the  $k$  most adjacent samples in the feature space.

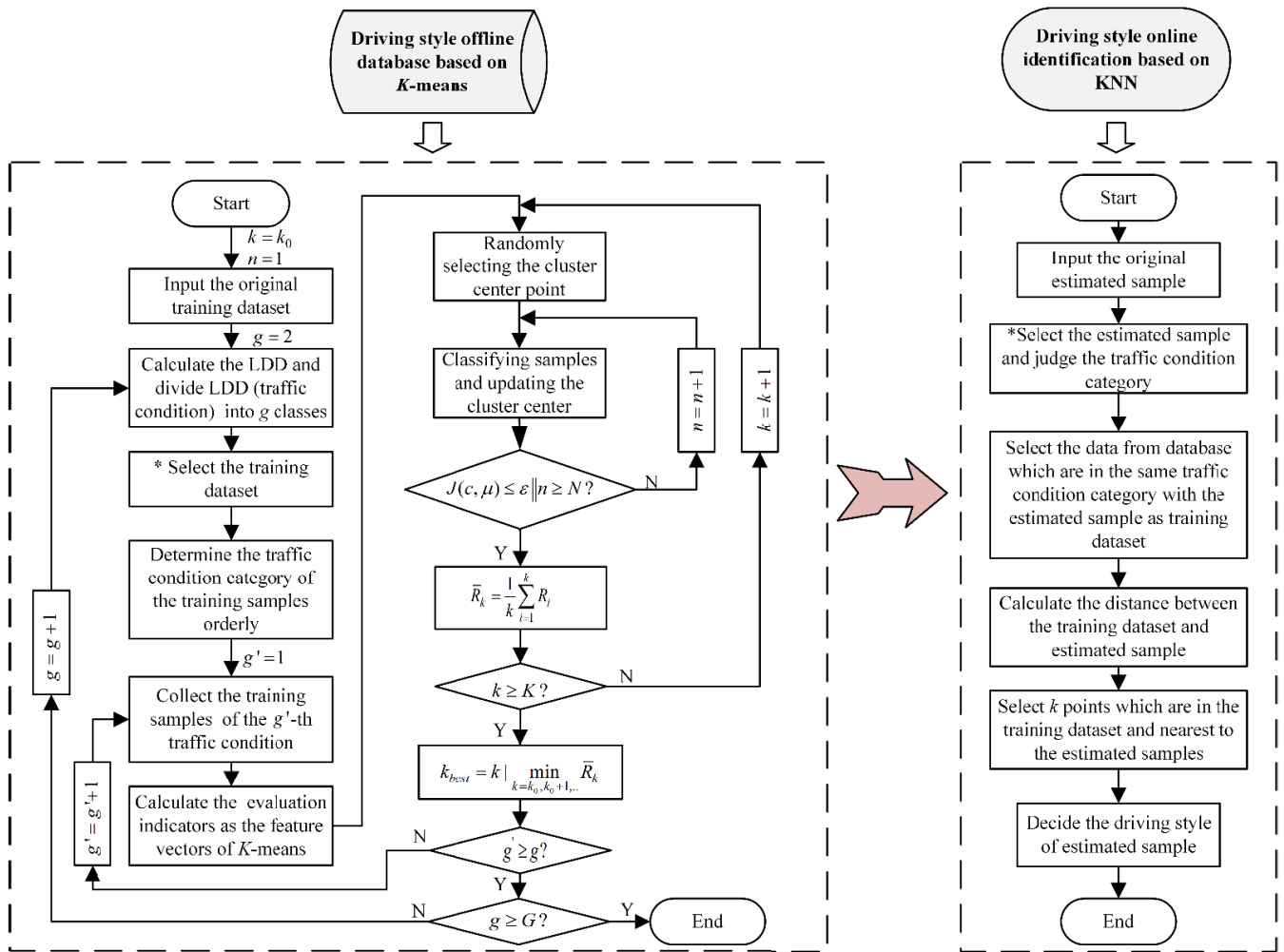


FIGURE 6. Framework of driving style determination.

The detailed flow is shown in the right side of Fig. 6, for more detailed, please refer to [23].

### C. LCD BEHAVIOR PREDICTION

#### 1) INPUT AND OUTPUT OF DP&DS-LCD MODEL

According to the existing researches, driver’s LC intention will last 1 s to 5 s [24], [25]. Since different drivers have different intension lengths. In order to capture the driver’s intention as much as possible, a time-window  $T'$  from 1 s to 5 s is adopted. Then the driver’s psychological field intensity before the LCD time  $t$  is composed of feature vectors with  $T'$  time length, which is a time series, and set it to  $E^t$ . The expression for  $E^t$  is defined as follows:

$$E^t = \{e^{t-T'}, e^{t-T'+r\Delta t}, e^{t-T'+2r\Delta t}, \dots, e^t\} \quad (17)$$

here  $\Delta t$  is the frequency of data acquisition,  $\Delta t \in [0.01, 1]s$ .  $r$  is the time step,  $r \in [1, T'/\Delta t - 1]$ .

Moreover, there are obvious differences in driver’s mental state between LCD process and CF stage. In order to capture the effect of driver’s psychological changes on LCD, three

features are extracted. They are respectively the average value of  $E^t$ , the psychological field intensity at the LCD time-point ( $e^t$ ), and the mean value of  $\Delta E^t$ . Here,  $\Delta E^t$  is the difference between  $E^{t-\Delta t}$  and  $e^t$ , which is a time series. The expression for  $\Delta E^t$  is as follows:

$$\Delta E^t = \{\Delta e^{t-T',t}, \Delta e^{t-T'+r\Delta t,t}, \Delta e^{t-T'+2r\Delta t,t}, \dots, \Delta e^{t-\Delta t,t}\} \quad (18)$$

with

$$\Delta e^{t-T',t} = e^{t-T'} - e^t \quad (19)$$

here  $\Delta e^{t-T',t}$  is the difference of psychological field intensity between time  $t - T'$  and time  $t$ .

Therefore, the model input are expressed as:

$$X = [\bar{E}^t, e^t, \Delta \bar{E}^t] \quad (20)$$

The output is expressed as  $Y = \{0, 1\}$ , where “0” denotes Lane-Keeping (LK) behavior, “1” denotes LC behavior.

2) gcFOREST ALGORITHM

The gcForest [26] algorithm is utilized to train and test the DP&DS-LCD model. Compared with other common deep learning algorithms, gcForest does not have high requirements on the number of samples and has high training efficiency, so it can be expanded easily. The gcForest method is composed of multi-grained scanning and cascade forest. Multi-grained scanning is a feature processing method which can transform features. Cascaded forest uses the pooling method of deep neural network, which can extract characteristic features efficiently.

1) Multi-grained Scanning: As the left of Fig. 7 illustrates, the raw features of the DP&DS-LCD model are 3-dimension. Suppose that the sliding window size is 2-dimension, then a 2-dimension truncated feature vector will be generated by the sliding window at each step, and it will produce two feature vectors corresponding to the window. The total vectors will be used to train a random forest (Forest A, as shown in Fig. 7) and a completely random forest (Forest B, as shown in Fig. 7), which can extract features of different classes, then the class vectors will be generated. Because the output of the DP&DS-LCD model is two categories, so finally all the class vectors will be connected into a transformed feature vector with 8-dimension. The transformed feature vector has higher dimension and enhanced representation compared with the raw feature vector.

2) Cascaded Forest: As shown on the right of Fig. 7, cascade forest adopts the structure of deep network, which inputs data from the front layer, and let the output as the input of next layer. Each level of forest all includes random forests and completely random forests. Using the transformed feature vector as the input of the first-level cascaded forest, then each forest will produce two class distributions. The estimated class distribution will be combined with the original feature vector, which is a new feature vector with 16-dimension. And the new feature vector will be used as the input for the next level of cascade forest. In order to reduce the risk of overfitting, the class vector of each forest is generated by k-fold cross validation.

The forests in the concerned level will generate their own estimates, which will be applied to estimate whether the current level is enough. And the final prediction results can be obtained by averaging these estimates of the same class and selecting the class with the maximum value. If the prediction result has no significant performance gain, which means the current number of levels is enough, and the training process could be terminated.

IV. EXPERIMENTS

In order to demonstrate that the DP&DS-LCD model is effective, the NGSIM database is used in the experiment. And this section contains three parts: database and data processing, model validation, and experiment results and analysis.

A. DATABASE AND DATA PROCESSING

The I-80 dataset from NGSIM database is applied to train and test the LCD model. The dataset was collected from seven lanes and included three periods: from 4:00 p.m. to 4:15 p.m., from 5:00 p.m. to 5:15 p.m., and from 5:15 p.m. to 5:30 p.m. The vehicles' trajectory data were collected by 0.1 s. The data filtering methods are as follows:

1) The LCD behavior of the passenger car is only studied. This is because the other two kinds of vehicles' LCD factors are different from the passenger car and the sample size is small.

2) Only vehicle data on lane 2, 3, 4, and 5 are used. Because the lane 6 and lane 7 are near the entrance of the ramp and many vehicles are forced to change lanes. Moreover, since lane 1 is a high-occupancy lane, the vehicles' movements on this lane are not considered.

3) The continuous LC data are excluded. Because any vehicle movement more than one lane is more likely a mandatory movement.

The most accurate method to label the LCD point is finding the continuous change point of lateral position by using the vehicle trajectory. However, this method is less efficient when marking mass of data. According to the existing research [27], in the first 5 s before the vehicle's lane ID changing, when the lateral velocity is larger than 0.6m/s for the first time, it will be marked as the LCD point. And the LCD time-point is represented as  $t_{LCD}$ . Then, based on the above LC intention time-window, the LCD data are the trajectories from time  $t_{LCD}-T'$  to time  $t_{LCD}$ . Moreover, to ensure the LK trajectories and LCD trajectories have the same time length and in similar traffic conditions, the trajectories from time  $t_{LCD}-2T'$  to time  $t_{LCD}-T'$  are labeled as LK samples. Finally, 802 LC samples and 701 LK samples are obtained.

Furthermore, in order to eliminate the possible influence of the non-uniform data dimension on the experimental results, minimum-maximum normalization processing is adopted for the original data.

B. MODEL VALIDATION

To verify the effectiveness of the DP&DS-LCD model, three comparative experiments are designed, including Gipps [1], fuzzy reasoning inference [5], and DBN model [10]. The input variables of the three LCD models are shown in Table 1. And the gcForest algorithm is used in the three comparison models on training phase.

TABLE 1. Input of the three LCD models.

Comparative Model	Model Input
Gipps	$v, d_{n,n+2}, d_{n,n+2}, \Delta v_{n+2,n-2}$
Fuzzy Inference	$d_{n,n+1}, d_{n,n+2}, d_{n,n-2}, d_{n,n+2} + d_{n,n-2}$
DBN	$v, \Delta v_{n,n+1}, \Delta v_{n,n+2}, \Delta v_{n,n-2}, d_{n,n+1}, d_{n,n+2}, d_{n,n-2}$

In order to guarantee that the training data and test data are disjoint, a cross validation is utilized to evaluate the model

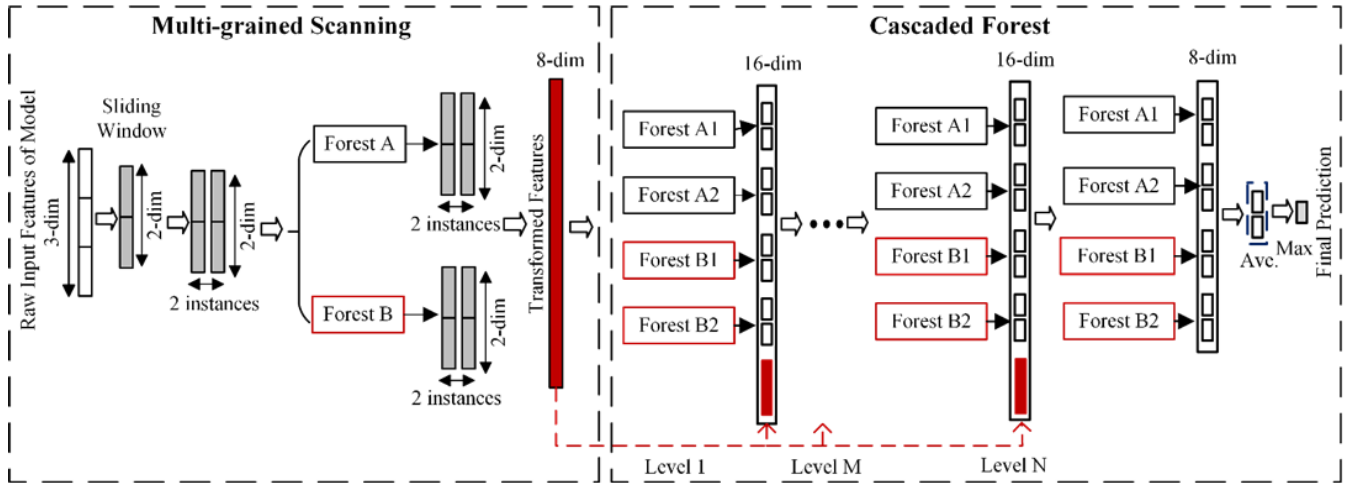


FIGURE 7. Overall illustration of gcForest algorithm.

performance. In this paper, each group of data is randomly divided into 10 folds, 9 folds will be used to train the model, and the other one fold will be applied to test the model effectiveness. The same procedure will be conducted 10 times. Accuracy, True Positive Rate (TPR) and False Positive Rate (FPR) are used to evaluate the prediction performance. The three evaluation indexes are calculated by (21).

$$\begin{aligned}
 Accuracy &= \frac{N_{TP} + N_{TN}}{N_P + N_N} \\
 TPR &= \frac{N_{TP}}{N_{TP} + N_{FN}} \\
 FPR &= \frac{N_{TN}}{N_{FP} + N_{TN}}
 \end{aligned} \tag{21}$$

where  $N_{TP}$ ,  $N_{TN}$ ,  $N_{FP}$ , and  $N_{FN}$  are the true positive, true negative, false positive, and false negative. This research labels the LC samples as positive samples, conversely, the LK samples are negative samples. The final experimental result is the average value of ten results.

### C. EXPERIMENT RESULTS AND ANALYSIS

The experimental results include two parts: driving style classification and LCD prediction results.

#### 1) DRIVING STYLE CLASSIFICATION RESULTS

The experimental data are randomly divided according to the ratio of 8:2. The first 80% of the data are adopted for the establishment of the driving style database, and the last 20% are used for the driving style identification. For simplifying, the LDD is divided into three categories by pre-equidistance. The previous studies mostly divided the driving styles into three categories [12], [13], [16], so the initial clustering number of driving styles  $k_0$  is set to 3. And the DB indexes of different driving style classification number are compared, the maximum classification number  $K$  is set as 8. The comparison results are shown in Fig. 8. It can be found that in the low and medium LDD, when the

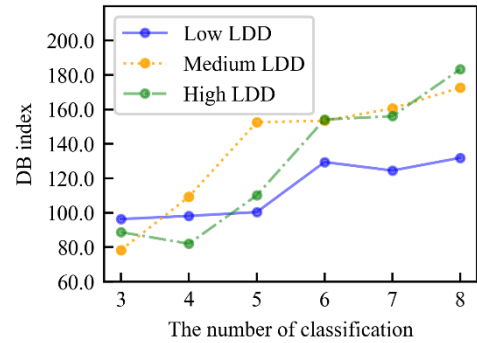


FIGURE 8. DB index of different classification numbers under the three traffic conditions.

classification number of driving styles is set to 3, the DB indexes all obtain the minimum value. For the high LDD, when the classification number is set to 4, the DB index gets the minimum value. However, if the class number is set to 4, the LC sample size of different driving styles will not meet the requirement of LC prediction. Therefore, for the high LDD, the classification number of driving styles is set to 3.

The comparisons of the three driving styles under different traffic conditions are shown in Fig. 9 and Fig. 10. In the two figures, ‘‘Cau.’’ represents the cautious drivers, ‘‘Neu.’’ represents the neutral drivers, and ‘‘Agg.’’ represents the aggressive drivers. As shown in Fig. 9, the speed on the three types of drivers is significantly different in the same traffic situation. Firstly, the speed distribution of different drivers varies greatly for a given traffic condition. Drivers with more aggressive style tend to have higher speed. Moreover, it finds that the speed distribution in different traffic conditions is in the different range, which reflects the differences of traffic states. These experimental results also prove the reliability of LDD proposed in this paper. In Fig. 10, it can also get the similar conclusion: drivers with more aggressive style also have higher acceleration under the same traffic condition.

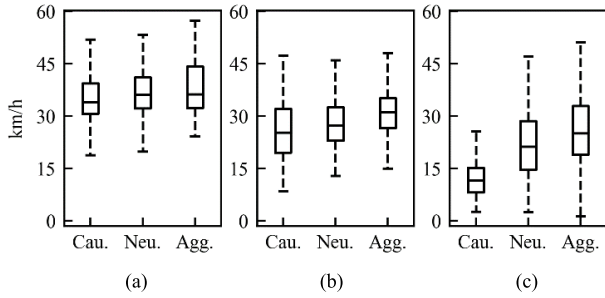


FIGURE 9. Box plots of driver's average speed distribution under different traffic conditions and driving styles. (a) Low LDD, (b) Medium LDD, (c) High LDD.

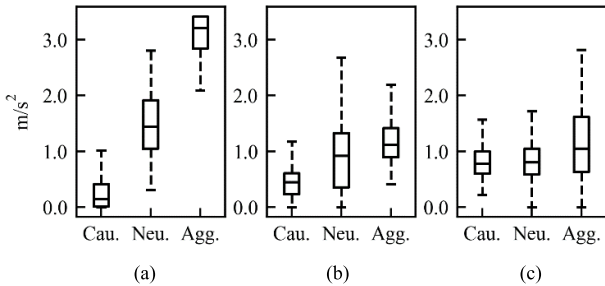


FIGURE 10. Box plots of driver's average acceleration distribution under different traffic conditions and driving styles. (a) Low LDD, (b) Medium LDD, (c) High LDD.

TABLE 2. Accuracy of DP&DS-LCD model (Unit: %).

Driving Style	Time Window				
	1s	2s	3s	4s	5s
Cautious	94.7	95.6	96.3	96.4	<b>96.7</b>
Neutral	96.4	93.5	98.2	98.2	<b>98.8</b>
Aggressive	96.5	97.1	<b>97.5</b>	96.1	96.3
Mean	95.9	95.4	97.3	96.9	97.3
Non-Classified	92.9	91.5	93.2	93.7	92.5

2) PREDICTION RESULTS OF DP&DS-LCD MODEL

Table 2 shows the prediction accuracy of DP&DS-LCD model under different time windows. In Table 2, the maximum accuracy obtained by the same driving style is bolded. For the cautious and neutral drivers, it finds that with the increasing of time-window size, the prediction results achieve the best at the 5 s time-window. And for aggressive drivers, the accuracy gets the best at the 3 s time-window. Moreover, the predicted accuracy after classification is significantly higher than that of unclassified data for different time windows.

Table 3 shows the prediction accuracies of the four models. And the maximum accuracy of each LCD model is bolded. Among them, the accuracy of DP&DS-LCD model is the average accuracy under the five time-windows. From Table 3, it can be found that the overall accuracy of DP&DS-LCD model is better than the other three models, whether for classified samples or non-classified samples. For a specified

TABLE 3. Accuracy of the four LCD models (Unit: %).

Driving Style	DP&DS-LCD	Gipps	Fuzzy Inference	DBN
Cautious	95.9(SD=0.65)	60.7	69.4	<b>63.3</b>
Neutral	<b>97.0(SD=1.77)</b>	<b>65.6</b>	71.1	60.0
Aggressive	96.7(SD=0.48)	60.2	<b>71.5</b>	60.7
Mean	96.6(SD=0.71)	62.2	70.7	61.3
Non-Classified	92.8(SD=0.68)	57.7	67.8	57.8

driving style, the average accuracy of DP&DS-LCD model is higher than 95%, whereas the Gipps model is from 60% to 66%, the fuzzy inference model is from 69% to 72%, and the DBN model is from 60% to 64%, which are lower than DP&DS-LCD model. For non-categorized data, it could also find that the accuracy of DP&DS-LCD model is superior to the other three models. Furthermore, it can also obtain the same conclusion with the Table 2: for the four LCD models, the accuracies after classification are higher than that of the unclassified samples.

TABLE 4. TPR values of the four LCD models (Unit: %).

Driving Style	DP&DS-LCD	Gipps	Fuzzy Inference	DBN
Cautious	97.2(SD=0.82)	<b>52.6</b>	57.4(↓)	<b>52.0</b>
Neutral	97.9(SD=0.50)	52.1	<b>64.7</b>	46.8(↓)
Aggressive	98.1(SD=0.40)	48.8	63.1	<b>52.0</b>
Mean	97.7(SD=0.34)	51.2	61.7	50.3
Non-Classified	<b>98.6(SD=0.94)</b>	46.9	60.0	46.9

TABLE 5. FPR values of the four LCD models (Unit: %).

Driving Style	DP&DS-LCD	Gipps	Fuzzy Inference	DBN
Cautious	95.2(SD=0.92)	67.2	<b>79.1</b>	<b>72.2</b>
Neutral	<b>96.2(SD=3.18)</b>	<b>76.9</b>	76.5	71.3
Aggressive	95.6(SD=1.06)	69.8	78.5	67.9
Mean	95.7(SD=1.14)	71.3	78.0	70.5
Non-Classified	87.9(SD=0.74)	66.6	74.2	66.9

The TPR and FPR values of the four models are shown in Table 4 and Table 5, where TPR is the prediction accuracy of LC samples and FPR is the prediction accuracy of LK samples. The down arrow (↓) is used to show the performance decrease of classified method compared with non-classified method. Attention, the TPR (FPR) value of DP&DS-LCD model refers to the mean value of TPR (FPR) under all time-windows. For DP&DS-LCD model, it finds that the prediction accuracy of LC behavior is slightly better than LK behavior. Similarly, whether TPR or FPR value, DP&DS-LCD model is all better than the other three models.

In addition, because gcForest algorithm is used in training the three comparative models, which may lead to the advantages of the comparative models are not be fully

reflected. Therefore, this paper compared the results of the original articles with the DP&DS-LCD model. Gipps [1] proposed the Gipps model, but they did not actually calibrate and verify the model through actual data. So the results of other two models in the original text are compared, which are the fuzzy reasoning model [5] and DBN model [10], as shown in Table 6.

**TABLE 6. Experimental results of the comparative models in the original papers.**

Indexes	DP&DS-LCD	Fuzzy Inference	DBN
LC Samples	802	334	1078
LK Samples	701	442337	1120
Accuracy (%)	96.6	/	99.3
TPR (%)	97.7	82.2	99.5
FPR (%)	95.7	97.0-99.5	99.1

For fuzzy reasoning model, the prediction accuracy of LC samples was 82.2%, and the accuracy of LK samples was from 97.0% to 99.5%. Although the accuracy of LK samples was slightly higher than DP&DS-LCD model, the accuracy of LC samples was severely lower than DP&DS-LCD model. So on the whole, DP&DS-LCD model get the better performance than fuzzy inference model.

Then, for DBN model, the overall prediction accuracy in the original article was 99.3%, with the values of TPR and FTR were 99.5% and 99.1% respectively. The prediction results of DP&DS-LCD model were slightly lower than the DBN model. However, it must note that the verification method of the two papers were different. The verification method of DBN model was dividing the training and test data according to the ratio of 8:2, and the final experimental results were the optimal results that can be achieved by the test set at one time. But this paper used the 10-fold cross validation, and the final results were the average of ten experiments. If the same verification method was adopted in this study, the final results may be better.

In conclusion, compared with Gipps model, fuzzy reasoning model, and DBN model, DP&DS-LCD model achieved the encouraging results. The average accuracy of DP&DS-LCD model was 96.6%, the average accuracy of LC samples was 97.7% and that of the LK samples was 95.7%. Additionally, the overall accuracy of DP&DS-LCD model improved from 92.8% to 96.6% after considering the driver's current driving style. The results of DP&DS-LCD model proved that it was meaningful to coupling DP and DS.

## V. CONCLUSION AND DISCUSSION

LCD behavior is mainly affected by the DP and DS. However, the present LCD researches mostly focused on the objective LC traffic conditions, few considered the DP and DS simultaneously. Therefore, a novel LCD model is developed in this research, which integrates the DP and DS, named DP&DS-LCD. In DP&DS-LCD model, psychological field model is developed to quantify the driver's psychology effect

of the surrounding vehicles on the driver. Then, a driving style classification model is developed, which includes the learning and recognition stage. This method could obtain the driver's current driving style. After that, the gcForest is adopted to train the DP&DS-LCD model. The gcForest algorithm can extract feature vectors effectively. Finally, the open I-80 dataset from NGSIM database was utilized for model validation. The experimental results showed that the clustering effect obtained the best when the driving styles were divided into cautious, neutral, and aggressive groups. It also found that the accuracy improved effectively after adding the real-time driving style into the LCD model. And the DP&DS-LCD model get encouraging results compared with the Gipps, fuzzy reasoning, and DBN model. In conclusion, the DP&DS-LCD model is verified to be effective.

Additionally, in V2V environment, DP&DS-LCD model could be utilized to predict the vehicles' LC behavior in real-time. Then, the prediction results can provide support for the automatic vehicles' decision. Moreover, this research can also enable the automatic vehicles to make human-like decisions in man-machine shared driving, which could improve driver's driving comfort. However, due to the length limitation of experimental road, the long-time individual trajectory data cannot be obtained. This may lead to inaccurate classification of driving styles. Therefore, the next work of this study is to use the driving simulator to obtain a relatively long-time trajectory data of individual vehicles, and still adopts the driving style classification method proposed in this paper. Taking the individual driver's historical trajectory data as the training samples, and analyzing the driving style that drivers present in different traffic circumstances, then judging the driver's current driving style. Thus, the final LCD prediction results may be better.

## REFERENCES

- [1] P. G. Gipps, "A model for the structure of lane-changing decisions," *Transp. Res. B, Methodol.*, vol. 20, no. 5, pp. 403–414, Oct. 1986.
- [2] M. T. Kind and A. Kesting, "Modeling lane-changing decisions with MOBIL," in *Proc. 7th Int. Conf. Traff. Granul. Flow (TFG)*, Paris, France, Jun. 2007, pp. 211–221.
- [3] J. Wang, Q. Zhang, D. Zhao, and Y. Chen, "Lane change decision-making through deep reinforcement learning with rule-based constraints," in *Proc. Int. Joint Conf. Neural Netw. (IJCNN)*, Budapest, Hungary, Jul. 2019, pp. 1–6.
- [4] S. Das and B. A. Bowles, "Simulations of highway chaos using fuzzy logic," in *Proc. 18th Int. Conf. NAFIPS*, New York, NY, USA, Jun. 1999, pp. 130–133.
- [5] E. Balal, R. L. Cheu, and T. Sarkodie-Gyan, "A binary decision model for discretionary lane changing move based on fuzzy inference system," *Transp. Res. C, Emerg. Technol.*, vol. 67, pp. 47–61, Jun. 2016.
- [6] S. Moridpour, M. Sarvi, G. Rose, and E. Mazloumi, "Lane-changing decision model for heavy vehicle drivers," *J. Intell. Transp. Syst.*, vol. 16, no. 1, pp. 24–35, Feb. 2012.
- [7] S. Coskun and R. Langari, "Predictive fuzzy Markov decision strategy for autonomous driving in highways," in *Proc. IEEE Conf. Control Technol. Appl. (CCTA)*, Copenhagen, Denmark, Aug. 2018, pp. 1032–1039.
- [8] W. Yuan, Z. Li, and C. Wang, "Lane-change prediction method for adaptive cruise control system with hidden Markov model," *Adv. Mech. Eng.*, vol. 10, no. 9, pp. 1–9, Sep. 2018.
- [9] X. Zhang, J. Sun, X. Qi, and J. Sun, "Simultaneous modeling of car-following and lane-changing behaviors using deep learning," *Transp. Res. C, Emerg. Technol.*, vol. 104, pp. 287–304, Jul. 2019.

- [10] D.-F. Xie, Z.-Z. Fang, B. Jia, and Z. He, "A data-driven lane-changing model based on deep learning," *Transp. Res. C, Emerg. Technol.*, vol. 106, pp. 41–60, Sep. 2019.
- [11] J. Gao, Y. L. Murphey, and H. Zhu, "Multivariate time series prediction of lane changing behavior using deep neural network," *Appl. Intell.*, vol. 48, no. 10, pp. 3523–3537, Oct. 2018.
- [12] X. Li, W. Wang, and M. Roetting, "Estimating driver's lane-change intent considering driving style and contextual traffic," *IEEE Trans. Intell. Transp. Syst.*, vol. 20, no. 9, pp. 3258–3271, Sep. 2019.
- [13] G. Ren, Y. Zhang, H. Liu, K. Zhang, and Y. Hu, "A new lane-changing model with consideration of driving style," *Int. J. Intell. Transp. Syst. Res.*, vol. 17, no. 3, pp. 181–189, Sep. 2019.
- [14] H. R. Eftekhari and M. Ghatee, "A similarity-based neuro-fuzzy modeling for driving behavior recognition applying fusion of smartphone sensors," *J. Intell. Transp. Syst.*, vol. 23, no. 1, pp. 72–83, Jan. 2019.
- [15] Y. Feng, S. Pickering, E. Chappell, P. Iravani, and C. Brace, "Driving style analysis by classifying real-world data with support vector clustering," in *Proc. 3rd IEEE Int. Conf. Intell. Transp. Eng. (ICITE)*, Singapore, Sep. 2018, pp. 264–268.
- [16] K.-T. Chen and H.-Y.-W. Chen, "Driving style clustering using naturalistic driving data," *Transp. Res. Record: J. Transp. Res. Board*, vol. 2673, no. 6, pp. 176–188, Jun. 2019.
- [17] K. Lewin, "Defining the 'field at a given time,'" *Psychol. Rev.*, vol. 50, no. 3, pp. 292–310, May 1943.
- [18] K. Amezcua-Semprun, P. Chen, W. Chen, and Z. Zhao, "The concept of stimuli-induced equilibrium point and its application in ramp-merging control," *IEEE Trans. Intell. Transp. Syst.*, vol. 19, no. 9, pp. 2814–2825, Nov. 2017.
- [19] P. Tao, "Modeling of driving behavior based on the psychology field theory," Ph.D. dissertation, School Transp., Jilin Univ., Changchun, China, 2012.
- [20] D. Yi, J. Su, C. Liu, M. Qudus, and W.-H. Chen, "A machine learning based personalized system for driving state recognition," *Transp. Res. C, Emerg. Technol.*, vol. 105, pp. 241–261, Aug. 2019.
- [21] S. Al-Sultan, A. H. Al-Bayatti, and H. Zedan, "Context-aware driver behavior detection system in intelligent transportation systems," *IEEE Trans. Veh. Technol.*, vol. 62, no. 9, pp. 4264–4275, Nov. 2013.
- [22] D. K. Roy and L. K. Sharma, "Genetic K-means clustering algorithm for mixed numeric and categorical data sets," *Int. J. Artif. Intell. Appl.*, vol. 1, no. 2, pp. 23–28, Apr. 2010.
- [23] X. Wu, V. Kumar, J. R. Quinlan, J. Ghosh, Q. Yang, H. Motoda, G. J. McLachlan, A. Ng, B. Liu, P. S. Yu, Z.-H. Zhou, M. Steinbach, D. J. Hand, and D. Steinberg, "Top 10 algorithms in data mining," *Knowl. Inf. Syst.*, vol. 14, no. 1, pp. 1–37, Jan. 2008.
- [24] E. Chung, H. Jung, E. Chang, and I. Lee, "Vision based for lane change decision aid system," in *Proc. Int. Forum Strategic Technol. (IFOST)*, Ulsan, South Korea, Oct. 2006, pp. 10–13.
- [25] N. Kauffmann, F. Winkler, F. Naujoks, and M. Vollrath, "What makes a cooperative driver identifying? Parameters of implicit and explicit forms of communication in a lane change scenario," *Transp. Res. F, Traffic Psychol. Behaviour*, vol. 58, pp. 1031–1042, Oct. 2018.
- [26] Z.-H. Zhou and J. Feng, "Deep forest: Towards an alternative to deep neural networks," in *Proc. IEEE 19th Int. Conf. Intell. Transp. Syst. (ITSC)*, Aug. 2017, pp. 3553–3559.
- [27] Y. Liu, X. Wang, L. Li, S. Cheng, and Z. Chen, "A novel lane change decision-making model of autonomous vehicle based on support vector machine," *IEEE Access*, vol. 7, pp. 26543–26550, 2019.



**CONG WU** received the bachelor's degree in transportation (planning and management) from Jilin University, Changchun, China, in 2014, where she is currently pursuing the master's degree with the School of Transportation. Her research interests include traffic flow theory and driving behavior.



**PENGFEE TAO** received the B.S. degree in computer science and technology, and the M.S. and Ph.D. degrees in traffic engineering from Jilin University, China. He is currently an Associate Professor with the School of Transportation, Jilin University. His research interests include driving behavior analysis and autonomous vehicles.



**JING TIAN** received the bachelor's degree in traffic engineering from Jilin University, Changchun, China, in 2014, where she is currently pursuing the master's degree with the School of Transportation. Her research interests include traffic condition prediction and deep learning.



**ZHIHUI LI** received the B.S. degree in computer science from the East China University of Metallurgy and the M.S. and Ph.D. degrees in computer software and theory from Jilin University, China. He is currently a Professor with the School of Transportation, Jilin University. His research interests include intelligent traffic systems, video detection and processing, and automatic driving.



**LIN MA** received the bachelor's degree in traffic engineering from Jilin University, Changchun, China, in 2013, and the master's degree from the School of Transportation, Jilin University, in 2017. His research interests include traffic signal control and traffic flow theory.

...